

Gas separation properties of aromatic polyamides with sulfone groups

K. Ghosal†, B. D. Freeman* and R. T. Chern‡

Department of Chemical Engineering, North Carolina State University, Raleigh,
NC 27695, USA

and J. C. Alvarez, J. G. de la Campa, A. E. Lozano and J. de Abajo

Instituto de Ciencia y Tecnologia de Polimeros, Juan de la Cierva 3, 28006 Madrid, Spain

(Received 20 April 1994)

The gas transport properties of three aromatic polyisophthalamides based on isophthaloyl chlorides and 4,4'-diaminodiphenylsulfone are reported at 35°C. The effects of bulky *t*-butyl and phthalimide substituents, at the 5 position of the isophthaloyl chloride moiety, on CO₂, CH₄, O₂, N₂, H₂ and He permeability, solubility and diffusivity were determined and correlated with chain packing and thermal properties of the polymers. Gas permeability was higher in substituted polyisophthalamides than in the unsubstituted analogue. Polymers containing the pendent *t*-butyl substituent have substantially higher permeability than polymers bearing the phthalimide substituent, despite the fact that the phthalimide substituent appears to be more bulky than the *t*-butyl group, based on van der Waals volume estimations. The strong polarity of the phthalimide moiety may act to increase chain-chain cohesive forces, which would tend to enhance chain packing, thereby reducing the packing-disrupting ability of the bulky phthalimide group. The permeability increase of the substituted polymers was accompanied by a permselectivity decrease.

(Keywords: aromatic polyamides; membrane gas separation; gas permeation)

INTRODUCTION

Membrane-based gas separation has emerged as a commercially important technology for replacement of, or use in combination with, traditional gas separation methods such as cryogenic distillation, pressure swing adsorption and amine absorption^{1,2}. Membranes are currently used industrially in applications such as hydrogen recovery from petrochemical recycle and purge gas streams, stripping of carbon dioxide from natural gas, and preparation of nitrogen-enriched air^{1,2}.

An important element contributing to gas separation technology success is the development of new membrane materials with high permeabilities and permselectivities. In this regard, considerable progress has been made in the elucidation of the influence of polymer structure on gas permeability and permselectivity. Typically, polymers with high permeabilities have low permselectivities and vice versa³. However, recent studies have chronicled remarkable success in enhancing *both* permeability and permselectivity through controlled, systematic variation of primary polymer chemical structure. The incorporation of bulky structural elements that simultaneously decrease both packing efficiency and torsional mobility can increase

gas permeability with only minimum selectivity losses⁴⁻⁹. Families of polysulfones^{4,5,10-17}, polycarbonates^{4,6,18,21} and polyimides^{9,22-25} have been optimized using this guideline.

This report documents an extension of this paradigm to aromatic polyisophthalamides (PIPAs). As a class, aromatic polyamides offer excellent thermal and mechanical properties, show good chemical resistance and are easily spun into hollow fibres appropriate for high-performance gas separation modules^{26,27}. Moreover, these materials have higher yield stress and modulus than polysulfone, a material widely used for membrane gas separation, and have extraordinarily high service temperatures (many approaching 300°C)²⁶.

The chemical structure of the family of amorphous polyisophthalamides selected for this study is presented in Table I. These polymers are based on the condensation of isophthaloyl chlorides (IPCs) and 4,4'-diaminodiphenylsulfone (DDSO). The effects of bulky *t*-butyl and phthalimide moieties (substituted at the 5 position in the diacid moiety) on gas permeation and separation characteristics were determined.


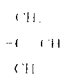
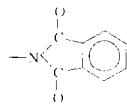
In general, polyamides exhibit high cohesive energy density, a strong propensity for very efficient polymer chain packing, and a semicrystalline morphology. For these reasons, they normally exhibit low gas permeability to small molecules²⁸. The aromatic polyamides in this study are amorphous since the backbones contain bulky non-collinear sulfone groups and a packing-disrupting

* To whom correspondence should be addressed.

† Present address: Reichhold Chemicals, Research Triangle Park, NC 27709, USA

‡ Present address: Merck Research Labs, WP 78-110, Sumneytown Pike, West Point, PA 19486, USA

Table 1 Chemical structures and physical properties of polyamides

							
Polymer code	X	T_g (°C)	Density (g cm ⁻³)	PD ^a	FFV ^b	d -spacing ^c (Å)	η ^d (dl g ⁻¹)
IP/SO2	H	323	1.378	3.25	0.100	4.6	1.01
TBI/SO2		337	1.269	3.17	0.110	4.8	1.32
PII/SO2		350	1.397	3.30	0.094	4.0	0.84

^a $PD = (V_f - V_w)/V_f$ ^b $FFV = (1 - 1.3V_w)/V_f$ ^c d -spacing from WAXD measurements^d Inherent viscosity in 0.5% NMP solution at 25 °C

meta-substituted acid. Moreover, the massive *t*-butyl and phthalimide substituents incorporated into the backbones of the polymers in this study may further disrupt chain packing and, therefore, increase gas permeability.

EXPERIMENTAL

Monomer and polymer synthesis

IPC and DDSO were purchased from commercial suppliers. IPC was purified by recrystallization from *n*-hexane and DDSO was recrystallized from water. *N,N*-Dimethylacetamide (DMAc), the polymerization solvent, was distilled twice over P₂O₅ at reduced pressure.

5-*t*-Butylisophthaloyl chloride (TBIC) was prepared from 5-*t*-butylisophthalic acid by refluxing it with excess SOCl₂ for 3 h. The product was recrystallized from hexane and had a melting point of 44 °C (lit.²⁹ 43 °C). 5-Phthalimidoisophthalic acid was synthesized by condensation of 5-aminoisophthalic acid and phthalic anhydride as previously reported³⁰. 5-Phthalimidoisophthaloyl chloride (PIIC) was prepared from the diacid by treatment with excess SOCl₂, and purified by recrystallization from *n*-hexane (m.p. 178 °C).

The following general procedure was used for polymer synthesis: First, 20 mmol of diacid chloride were added slowly to a stirred solution containing 20 mmol of diamine in 40 ml of DMAc at 0 °C. The mixture was allowed to react under a blanket of nitrogen for 2 h, then the temperature was raised to 20 °C, and the reaction allowed to proceed for a further 2 h. The solution was cooled to 0 °C and a small excess (0.2 mmol) of diacid chloride was added. Finally, the reactants were held at room temperature for 2 h. The viscous polymer solution was poured into a flask containing distilled water, and the polymer was filtered off, washed several times with water, extracted with acetone in a Soxhlet extractor for 24 h and finally dried in a vacuum oven at 100 °C overnight. Yields of over 95% were obtained. Monomer and polymer primary chemical structure was verified by FTIR and ¹H n.m.r. spectroscopy.

Film preparation

IP/SO2 and TBI/SO2 films (see Table 1 for polymer codes) were prepared by casting a 10% (w/v) *N,N*-dimethylacetamide (DMAc) solution on a flat glass plate, which was then placed in an oven. PII/SO2 was insoluble in DMAc and was, therefore, cast from a 1/1 (v/v) mixture of DMAc and *N,N*-dimethylformamide (DMF). The solutions were filtered through a Gelman[®] 1 µm glass-fibre filter to remove any particulates that could lead to a defect in the film. The film was dried on a glass plate for 48 h at 100 °C and atmospheric pressure. The glass plate was then removed from the oven, cooled and the film lifted from the plate. After the film was air dried, it was annealed in a vacuum oven at 160 °C for 48 h. No trace of solvent could be detected from differential scanning calorimetry (d.s.c.) scans, and no indications of crystallinity were observed in d.s.c. scans or wide-angle X-ray diffraction (WAXD) spectra. All films were between 1 and 2 mil (25–50 µm) thick.

Since IP/SO2 and TBI/SO2 films were cast from DMAc, and PII/SO2 from a 1/1 mixture of DMAc and DMF, an experiment was carried out to determine the influence of casting solvent on gas transport properties. IP/SO2 was cast from a 1/1 mixture of DMAc and DMF and given the same thermal protocol as IP/SO2 cast from DMAc. The permeability of IP/SO2 to CO₂, the most soluble penetrant considered in this study, was independent of casting solvent, as shown later in Figure 1.

Thermal characterization

Glass transition temperatures were determined using a Perkin–Elmer DSC-7 at a heating rate of 20 °C min⁻¹. The samples were scanned twice and the midpoint of the endothermal displacement of the second scan was taken to be the T_g .

Physical characterization

Polymer density was determined by flotation of small film samples in a density gradient column, which was maintained at 23 ± 0.1 °C. Aqueous solutions of zinc

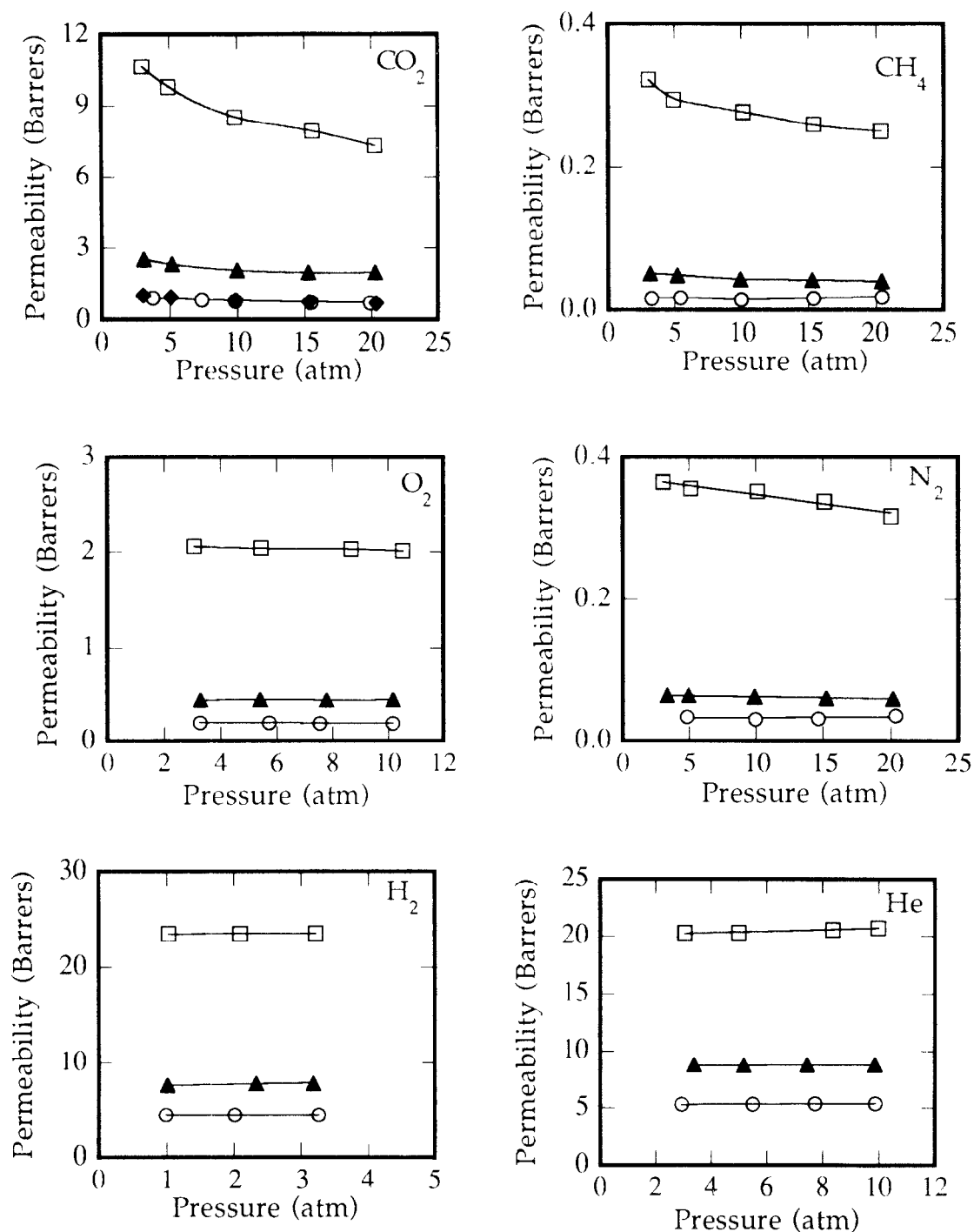


Figure 1 The effect of upstream pressure on permeability at 35 °C: (○) IP/SO₂; (□) TBI/SO₂; (▲) PII/SO₂; (◆) IP/SO₂ cast from 1:1 (v/v) mixture of DMAc and DMF

chloride or sodium bromide provided the gradient. Glass beads, whose densities are known to $\pm 0.0001 \text{ g cm}^{-3}$, were used to calibrate the column. A similar methodology was used previously to determine the densities of aromatic polyamides²⁸.

The density data were used to characterize chain packing by estimating the fractional free volume (FFV), which was calculated using the following relation³¹:

$$FFV = \frac{V - 1.3V_w}{V} \quad (1)$$

where V is the polymer specific volume, and V_w is the specific van der Waals volume calculated using the group

contribution method of Bondi^{32,33}. The packing density (PD), which is a related measure of chain packing, was calculated using⁷:

$$PD = \frac{V}{V - V_w} \quad (2)$$

WAXD spectra were obtained with a Siemens WAXD spectrometer, using Cu K α radiation, which has a wavelength of 1.54 Å. The d -spacing was calculated from Bragg's equations, $d = \lambda / 2 \sin \phi$, where λ is the wavelength of the radiation and 2ϕ is the angle of maximum intensity in the amorphous halo exhibited by these polymers.

Inherent viscosities of all polymer samples were

determined in 0.5% *N*-methyl-2-pyrrolidinone solutions at $25 \pm 0.1^\circ\text{C}$ in an automated Ubbelohde viscometer.

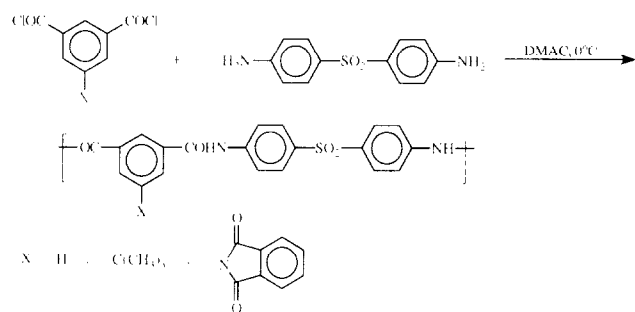
Gas permeability determination

A barometric permeation method was used to determine steady-state pure gas permeability at 35°C over a range of pressures up to 20 atm³⁴. The downstream pressure was kept below 10 mmHg, while the upstream pressure was maintained at super-atmospheric pressures. CO_2 , O_2 and H_2 were purchased from Linde, N_2 and He from National Specialty Gases, and CH_4 from Air Products. CH_4 and O_2 had a purity of $>99.5\%$; all other gases had a purity of $>99.99\%$. All permeability determinations were performed on films that had first been 'vector conditioned' with CO_2 at 20 atm³⁵. Effective gas diffusivities were estimated from time-lag data at an upstream pressure of 3 atm using the relation $D = l^2/6\theta$, where l is film thickness and θ is the time lag³⁶. The apparent solubility coefficient of each gas was estimated from the relation³⁶ $S = P/D$. Time lags for H_2 and He were too short to permit accurate determination of the diffusion coefficient. For safety reasons, O_2 and H_2 permeabilities were not determined at high pressures.

RESULTS AND DISCUSSION

Polymer synthesis and characterization

Aromatic polyisophthalamides containing sulfone groups were prepared from DDSO and three diacid chlorides based on IPC by the low-temperature polycondensation method in DMAc. The reaction is depicted in Scheme 1. The polymers were obtained in virtually



Scheme 1

quantitative yield and, once purified, they were identified by spectroscopic methods. The polymers were soluble in aprotic polar solvents (such as DMAc and NMP) and tough, transparent films could be fabricated by evaporation of cast solutions, as described in the 'Experimental' section. All three polymers showed high inherent viscosities (IV), around 1.0 dl g^{-1} , which correspond to comparatively high-molecular-weight polymer.

Substituted PIPAs have higher glass transition temperatures than the unsubstituted analogue (IP/SO2), as indicated by T_g data presented in Table 1. These results are consistent with the notion that the addition of bulky substituents to polymer backbones can act to inhibit local-scale segmental polymer dynamics important in the glass-rubber transition and, therefore, increase T_g values³⁷. Moreover, glass transition temperatures also tend to increase as polymer cohesive energy density

increases³⁷. The polymer prepared with the bulky, non-polar *t*-butyl substituent has a T_g that is 14°C higher than the unsubstituted analogue. The phthalimide-substituted polymer has a T_g that is 27°C higher than that of the unsubstituted IP/SO2. As the phthalimide substituent is both bulky and highly polar, it could act to increase T_g by two mechanisms: (1) inhibiting backbone mobility, like the *t*-butyl substituent, and (2) increasing polymer chain-chain cohesive energy density due to the very polar nature of the substituent. In fact, similar behaviour has been observed for PIPAs containing other bulky, polar pendent heterocycles, such as benzoxazole and benzothiazole^{38,39}.

WAXD properties

The WAXD spectra of the PIPAs exhibit a broad halo, which is typical of amorphous polymers⁴⁰. The position of the halo is characterized by a d -spacing value, and the PIPA d -spacing values are presented in Table 1. TBI/SO2 has the largest d -spacing, followed by IP/SO2 and PII/SO2.

X-ray diffraction d -spacings of amorphous polymers have often been used to estimate average intersegment spacing (i.e. chain packing) in polymer matrices^{5,6,16,17}. However, recent theoretical studies of WAXD spectra from amorphous polymers suggest that the amorphous halo arises due to coherent intersegmental and intra-segmental diffraction of X-rays⁴⁰. If intersegmental scattering dominates the observed signal, then WAXD spectra can provide a sensitive probe of chain packing in the amorphous polymer. However, if intrasegmental scattering is dominant, then WAXD is not sensitive to interchain spacing. In the PIPAs under consideration, the relative importance of intersegmental and intra-segmental contributions to the observed WAXD spectra are not known. Therefore, these X-ray data are not assumed to be indicative of interchain spacing and only confirm the d.s.c. results, which indicate no detectable crystalline order in these polymers.

Gas transport

Figure 1 presents permeabilities of the polymers to CO_2 , CH_4 , N_2 , O_2 , H_2 and He at 35°C as a function of upstream pressure. TBI/SO2 is 4–20 times more permeable than IP/SO2, depending on the gas being considered. PII/SO2 is also more permeable than IP/SO2 but less permeable than TBI/SO2. Often, bulky backbone substituents, such as those present in TBI/SO2 and PII/SO2, disrupt chain packing in polymers, thereby increasing free volume and, in turn, permeability^{4–9}.

Over the pressure range probed in these studies, none of the polymers exhibits gas-induced plasticization, which would be signalled by an increase in permeability with increasing pressure. Typically, CO_2 is used as a probe of gas-induced plasticization since CO_2 is often the most soluble gas examined in a gas transport study, and the propensity of a penetrant to plasticize a polymer increases as the amount of penetrant dissolved in the polymer increases^{1,2}. Resistance to plasticization is an important property of membrane materials, particularly in high-pressure applications, such as CO_2 stripping from natural gas streams, since plasticized polymers exhibit markedly reduced selectivity to penetrant mixtures^{1,2}.

Table 2 provides a summary of permeability and permselectivity values at 35°C and 10 atm, while Table 3

Table 2 Permeabilities^a at 10 atm pressure and 35 °C

	P_{He}	$P_{\text{H}_2}^b$	P_{O_2}	P_{N_2}	P_{CO_2}	P_{CH_4}	$\frac{P_{\text{CO}_2}}{P_{\text{CH}_4}}$	$\frac{P_{\text{O}_2}}{P_{\text{N}_2}}$	$\frac{P_{\text{H}_2}^b}{P_{\text{CH}_4}}$
IP/SO2	5.2	4.3	0.19	0.03	0.78	0.014	56	6.3	307
TBI/SO2	20.7	23.5	2.0	0.37	8.6	0.27	32	5.4	87
PII/SO2	9.9	7.7	0.44	0.06	2.1	0.04	52	7.3	193

^a Permeabilities in barrers, 1 barrer = $\frac{10^{-10} \text{ cm}^3(\text{STP}) \text{ cm}}{\text{cm}^2 \text{ s cmHg}}$

^b P_{H_2} at 3 atm

Table 3 Diffusivities^a and solubilities^b at 3 atm pressure and 35 °C

	S_{O_2}	S_{CO_2}	$\frac{S_{\text{O}_2}}{S_{\text{N}_2}}$	$\frac{S_{\text{CO}_2}}{S_{\text{CH}_4}}$	D_{O_2}	D_{CO_2}	$\frac{D_{\text{O}_2}}{D_{\text{N}_2}}$	$\frac{D_{\text{CO}_2}}{D_{\text{CH}_4}}$
IP/SO2	0.56	7.5	1.0	6.1	0.26	0.09	6.5	9.0
TBI/SO2	0.60	9.4	1.1	3.7	2.6	0.86	5.2	8.6
PII/SO2	0.26	4.8	1.7	11	1.3	0.40	3.9	4.4

^a $D \times 10^8$ ($\text{cm}^2 \text{ s}^{-1}$) estimated from time-lag measurements at 3 atm

^b $S \left(\frac{\text{cm}^3(\text{STP})}{\text{cm}^3 \text{ polymer atm}} \right)$ calculated from $S = P/D$

presents gas solubilities, diffusivities, diffusivity selectivities and solubility selectivities for all polymers at 35 °C and 3 atm. From Table 2, for the hydrogen/methane gas pair, IP/SO2 is the most selective polymer, followed by PII/SO2, and TBI/SO2 exhibits the lowest selectivity. The permeability values are in the opposite order: TBI/SO2 > PII/SO2 > IP/SO2. This trend is consistent with the commonly observed trade-off between permeability and permselectivity: polymers that are more permeable tend to exhibit lower permselectivities and vice versa³. Changes in helium permeability with polymer structure are quite similar to the changes observed for hydrogen permeability. Since permeability to helium is typically similar to that of hydrogen, helium is often used, particularly at high pressure, as a surrogate penetrant for hydrogen, since hydrogen may present an explosion danger at high pressure.

For the oxygen/nitrogen gas pair, PII/SO2 is both more permeable and more selective than the unsubstituted analogue, IP/SO2, as indicated from the data presented in Table 2. From the values in Table 3, the higher permeability of PII/SO2 relative to IP/SO2 appears to be related to larger gas diffusion coefficients in PII/SO2. The higher selectivity of PII/SO2 relative to IP/SO2 is the result of a large increase in solubility selectivity in PII/SO2 coupled with a moderate decrease in diffusivity selectivity. O₂/N₂ solubility selectivity has been observed to increase as carbonyl concentration increases in a family of polycarbonates⁶. However, a detailed description of the molecular phenomena that couple polar carbonyl group concentration and O₂/N₂ solubility selectivity was not presented. The relationship between the chemical structure, packing of the polymer chains and the observed permeability/selectivity properties may also be related to subtle differences in size and distribution of both equilibrium and non-equilibrium molecular-scale 'gaps' or free volume in the polymer, which are required for gas solubility and diffusion^{1,2}.

TBI/SO2 exhibits the highest oxygen and nitrogen permeability and the lowest permselectivity of the three polymers investigated. This result is consistent with the notion that the bulky, non-polar *t*-butyl group acts to frustrate chain packing, thereby increasing polymer free volume and, in turn, gas diffusion coefficients in TBI/SO2 relative to the base polymer, IP/SO2. From the data presented in Table 3, oxygen diffusivity in TBI/SO2 is approximately 10 times that in IP/SO2. As explained in more detail later, this result is consistent with calculated fractional free-volume values reported in Table 1; the free volume of TBI/SO2 is greater than that of IP/SO2, and gas diffusion coefficients are commonly understood to be quite sensitive to polymer free volume. Oxygen solubility and solubility selectivity are slightly larger in TBI/SO2 than in IP/SO2. This result is consistent with the higher free volume in TBI/SO2. The low permselectivity of TBI/SO2 is consistent with the permeability/permselectivity trade-off discussed in the previous paragraph.

From Table 2, carbon dioxide permeability follows the same trend with chemical structure as the other gas pairs discussed previously, with the permeability of TBI/SO2 to CO₂ being substantially greater than that of PII/SO2, which is, in turn, greater than that of the base material, IP/SO2. The permselectivity of the CO₂/CH₄ gas pair decreases by approximately 8% with the addition of the bulky, polar phthalimide group to the chain backbone. This small change in permselectivity between IP/SO2 and PII/SO2 is a result of a strong decrease in CO₂/CH₄ diffusivity selectivity coupled with a large increase in CO₂/CH₄ solubility selectivity as presented in Table 3. These effects may be due to the very polar nature of the phthalimide group and the potential favourable electrostatic interactions between this group and CO₂ molecules. CO₂/CH₄ solubility selectivity is known to increase markedly as the concentration of polar carbonyl and sulfone groups in the polymer increases, presumably due to dipole-induced dipole (i.e. electrostatic) interactions between these polar groups and CO₂ (ref. 41). CO₂, being quadrupolar, can participate in such favourable electrostatic interactions while methane, being non-polar, cannot. Therefore, the higher CO₂/CH₄ solubility selectivity in PII/SO2 relative to IP/SO2 can be rationalized on the basis of the higher concentration of polar moieties in PII/SO2. Moreover, if the interaction of CO₂ with the polar groups is sufficiently strong, the mobility of CO₂ (relative to the mobility of non-polar CH₄) could be retarded in the more polar matrix, which could explain the lower diffusivity selectivity of PII/SO2 relative to IP/SO2.

The high permeability of TBI/SO2, relative to IP/SO2, to all gases results mainly from markedly higher

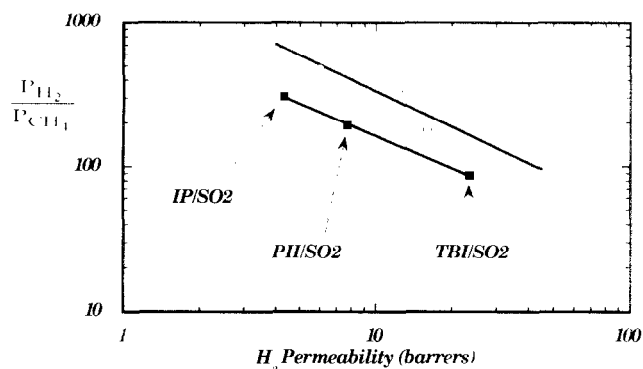


Figure 2 A comparison of hydrogen separation performance of aromatic polyamides prepared for this study (■), those used commercially²⁶ (○) and the 'upper bound' defined by Robeson³ (---)

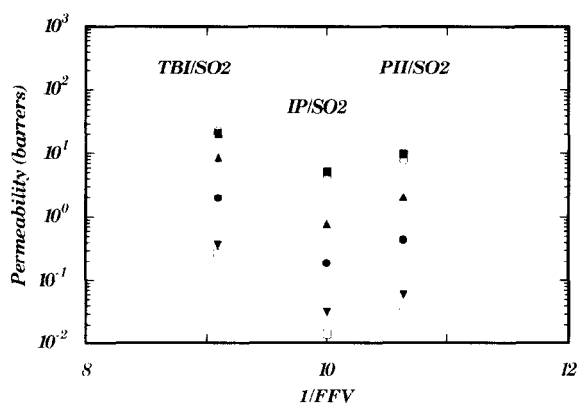


Figure 3 The dependence of gas permeabilities at 35 °C and 10 atm on fractional free volume: (■) He, (○) H₂, (▲) CO₂, (□) CH₄, (●) O₂, (▼) N₂

diffusivity values in TBI/SO₂, as presented in Table 3. For example, the diffusion coefficients of oxygen and carbon dioxide are approximately one order of magnitude greater in TBI/SO₂ than in IP/SO₂. The bulky t-butyl group presumably disrupts chain packing, thereby increasing *FFV* and, in turn, gas diffusivity. The increase in permeability is, however, accompanied by a rather important loss in selectivity. PII/SO₂, containing the bulky, polar phthalimide substituent, exhibits lower gas solubility than either of the other two polymers. However, PII/SO₂ has gas diffusion coefficients substantially greater than those observed in IP/SO₂ and somewhat less than those observed in TBI/SO₂. The overall combination of solubility and diffusivity leads to permeability values between those of IP/SO₂ and TBI/SO₂.

To understand better the trade-off between permeability and permselectivity, hydrogen permeability is presented as a function of H₂/CH₄ selectivity for the polymers in this study and other polymers in Figure 2. These particular data were selected because the recovery of hydrogen from hydrocarbon-containing process streams is important in chemical and petrochemical applications. The performance of these materials is compared with the performance of a series of proprietary commercial gas separation materials based on aromatic polyamides²⁶ and the 'upper bound' defined by Robeson³. The upper bound denotes current selectivity/permeability limits and has been defined by a careful examination of much of the existing published gas transport data. The polyamides prepared for this study fall below both the upper bound

and the commercial materials. They are, however, superior to first-generation commercial gas separation materials such as polysulfone. Moreover, the preparation of a successful commercial gas separation membrane depends on factors such as mechanical properties, high service temperatures, and ability to process the polymer into either asymmetric hollow fibres or thin-film composite membranes¹. In this regard, the materials under consideration in this study exhibit excellent mechanical and thermal properties and are amenable to solvent processing, a common route in the formation of asymmetric hollow fibres or thin-film composite membranes.

Free-volume analysis

Gas diffusivity *D* is often assumed to depend on free volume as described by the Fujita relationship³¹:

$$D = A \exp\left(-\frac{B}{FFV}\right) \quad (3)$$

where *A* and *B* are constants characteristic of the polymer-penetrant system. This relation typically provides a good description of gas diffusivity in a family of polymers^{17,31}. Lee³¹ proposed that solubility would not be a strong function of free volume and, therefore, that gas permeability *P* and *FFV* should be related by:

$$P = A' \exp\left(-\frac{B'}{FFV}\right) \quad (4)$$

where *A'* and *B'* are constants. The ease of *FFV* estimation makes this a useful relationship. As explained earlier, the *FFV* can be calculated from density data and estimations of van der Waals volume (*V_w*) by a group contribution method. The values of estimated fractional free volume for the polymers in this study are presented in Table 1.

TBI/SO₂ has a higher *FFV* value than IP/SO₂, consistent with the notion that bulky t-butyl pendent groups disrupt chain packing. Based on the free-volume calculations presented in Table 1, PII/SO₂ appears to pack more efficiently than its unsubstituted analogue, IP/SO₂, even though the polar phthalimide (PI) group is presumed to be quite bulky based on its van der Waals volume. However, strong attractions observed in polyimides are due in part to the interactions between imide rings, which can even give rise to charge-transfer complexes⁴². Addition of highly polar substituents to polysulfone has been found to decrease *FFV* as well, suggesting that any potential increase in *FFV* due to packing-disrupting bulky substituents is overridden by the increase in cohesive energy density accompanying the addition of polar groups to the chain backbone⁴³.

Figure 3 presents the dependence of gas permeability on *FFV* for this family of aromatic polyamides. While TBI/SO₂, the most permeable polymer considered in this study, has the highest fractional free volume, PII/SO₂ is 2–3 times more permeable than IP/SO₂ even though the calculated *FFV* of PII/SO₂ is lower than that of IP/SO₂. This observation may result from an artifact in the estimation of the van der Waals volume of IP/SO₂. Small errors in the estimation of *V_w* have been found to lead to large differences in calculated *FFV*^{28,44}. In the polymers considered in this study, an increase in *V_w* of IP/SO₂ of less than 2% would make this polymer's permeability values fall on a straight line with the other

two polymers in Figure 3. Moreover, the van der Waals volume of the structural elements used in the group contribution estimation of V_w is presumed to be independent of the chemical environment of the structural element. According to Bondi³², this assumption is good for heavy atoms, but not for smaller atoms like hydrogen and fluorine or for cases where strong association, such as hydrogen bonding, is present. Since polyamides are known to hydrogen-bond, some error in the estimate of V_w may be expected, which could affect free-volume calculations. Finally, gas permeability depends on solubility and diffusivity, and both factors cannot be understood by free-volume arguments alone⁴⁴.

Segmental mobility

Polymer segmental mobility can be restricted by incorporating bulky rigid groups on the polymer backbone, by destroying the rotational symmetry about the main-chain axis (e.g. by using *meta*-substituted phenyl groups instead of *para*-substituted phenyl groups), or by replacing flexible moieties in the main chain with rigid groups¹. In polyamides, the amide linkage is very rigid owing to the extensive resonance conjugation between the nitrogen and the carbonyl group, which imposes a partial double-bond character to the amide linkage⁴⁵. Since the nitrogen-carbonyl bond lacks a rotational axis, motion about it would involve cooperative motion of many segmental units. The motion of the *meta*-substituted phenyl ring in the diacid group is also severely restricted since it lacks a rotational axis; moreover, in the modified polymers, this ring is laden with mobility-reducing bulky substituents.

The groups with the largest degrees of rotational freedom are the phenyl rings in the diamine entity. These phenyl groups presumably undergo π flips similar to those observed in other glassy amorphous polymers, such as polycarbonate⁴⁶⁻⁴⁸. However, these polymers are high- T_g materials. Thus, although the phenyl rings linked to the $-\text{SO}_2-$ moiety certainly do not provide the chain rigidity of wholly aromatic polyamides, they are relatively rigid-chain polymers owing to the high potential barrier for phenyl ring rotation. In fact, the small value of the angle C-S-C of the diphenylsulfone unit (100.4°) is responsible for the higher energy for the rotation of the phenyl rings relative to other diamines with, for instance, $-\text{O}-$, $-\text{CH}_2-$, $-\text{S}-$ as hinge linkages^{49,50}. On the other hand, the permeabilities found for the current series of PIPAs are much higher than those of *para*-oriented aromatic polyamides of the Kevlar[®] type²⁸ or fully aromatic polyamides that do not have a 'hinge' linkage between the two phenylene rings of the diamine moiety and exhibit much more efficient chain packing than the PIPAs. Thus, this series of *meta*-oriented polyamides are, as a group, more permeable to gases than commercial *para*-oriented polyamides.

SUMMARY AND CONCLUSIONS

This study investigates the suitability of aromatic polyamides as potential membrane materials for gas separation. Polymers bearing bulky, non-polar *t*-butyl substituents are substantially more permeable than unsubstituted analogues. Polymers containing bulky, polar phthalimide substituents are found to be more permeable than the unsubstituted analogue but less

permeable than the *t*-butyl-substituted material. For most gases in these polymers, permselectivity decreases as gas permeability increases. This family of polymers offers attractively high service temperatures for membrane applications and appears to be amenable to structural fine tuning to achieve rational tailoring of gas permeation and separation properties.

ACKNOWLEDGEMENTS

This research was supported by the National Science Foundation (CTS-8903999-01 and CTS-9257911), the Ford Motor Company and 3M Company. We also thank the Spanish Comision Interministerial de Ciencia y Tecnologia (MAT92-0198) and the enterprise Proyectos S.A. for financial support. We thank Dr Jack Preston for many helpful suggestions and advice related to the synthesis and properties of polyamides. The technical assistance of Mr Andrew Metters in density determinations and Mr Atsushi Morisato in X-ray diffraction measurements is also appreciated.

REFERENCES

- 1 Koros, W. J. and Fleming, G. K. *J. Membr. Sci.* 1993, **83**, 1
- 2 Ghosal, K. and Freeman, B. D. *Polym. Adv. Technol.* 1994, **5**(11), 673
- 3 Robeson, L. M. *J. Membr. Sci.* 1991, **62**, 165
- 4 Moe, M. B., Koros, W. J. and Paul, D. R. *J. Polym. Sci., Polym. Phys. Edn.* 1988, **26**, 1931
- 5 McHattie, J. S., Koros, W. J. and Paul, D. R. *Polymer* 1991, **32**, 840
- 6 Hellums, M. W., Koros, W. J., Husk, G. R. and Paul, D. R. *J. Membr. Sci.* 1989, **46**, 93
- 7 Chern, R. T., Sheu, F. R., Jia, L., Stannett, V. T. and Hopfenberg, H. B. *J. Membr. Sci.* 1987, **35**, 103
- 8 Chern, R. T., Jia, L., Shimoda, S. and Hopfenberg, H. B. *J. Membr. Sci.* 1990, **48**, 333
- 9 Coleman, M. R. and Koros, W. J. *J. Membr. Sci.* 1990, **50**, 285
- 10 Aitken, C. L., Koros, W. J. and Paul, D. R. *Macromolecules* 1992, **25**, 3424
- 11 Aitken, C. L., Koros, W. J. and Paul, D. R. *Macromolecules* 1992, **25**, 3651
- 12 Aitken, C. L., Paul, D. R. and Mohanty, D. K. *J. Polym. Sci., Polym. Phys. Edn.* 1993, **31**, 983
- 13 Aitken, C. L. and Paul, D. R. *J. Polym. Sci., Polym. Phys. Edn.* 1993, **31**, 1061
- 14 Ghosal, K., Chern, R. T. and Freeman, B. D. *J. Polym. Sci., Polym. Phys. Edn.* 1993, **31**, 891
- 15 Ghosal, K. and Chern, R. T. *J. Membr. Sci.* 1992, **72**, 91
- 16 McHattie, J. S., Koros, W. J. and Paul, D. R. *Polymer* 1991, **32**, 2618
- 17 McHattie, J. S., Koros, W. J. and Paul, D. R. *Polymer* 1992, **33**, 1701
- 18 Aguilar-Vega, M. and Paul, D. R. *J. Polym. Sci., Polym. Phys. Edn.* 1993, **31**, 991
- 19 Muruganandam, N. and Paul, D. R. *J. Membr. Sci.* 1987, **34**, 185
- 20 McHattie, J. S., Koros, W. J. and Paul, D. R. *J. Polym. Sci., Polym. Phys. Edn.* 1991, **29**, 731
- 21 Hellums, M. W., Koros, W. J. and Schmidhauser, J. C. *J. Membr. Sci.* 1992, **67**, 75
- 22 Kim, T. H., Koros, W. J. and Husk, G. R. *Separ. Sci. Technol.* 1988, **23**, 1611
- 23 Kim, T. H., Koros, W. J., Husk, G. R. and O'Brien, K. C. *J. Membr. Sci.* 1988, **37**, 45
- 24 Stern, S. A., Mi, Y., Yamamoto, H. and St Clair, A. K. *J. Polym. Sci., Polym. Phys. Edn.* 1989, **27**, 1887
- 25 O'Brien, K. C., Koros, W. J. and Husk, G. R. *J. Membr. Sci.* 1988, **35**, 217
- 26 Ekiner, O. M. and Vassilatos, G. *J. Membr. Sci.* 1990, **53**, 259

- 27 Preston, J. in 'Aromatic Polyamides' (Eds. H. F. Mark, N. M. Bikales, C. G. Overberger, G. Menges and J. I. Kroschwitz, Wiley-Interscience, New York, 1988
- 28 Weinkauff, D. H., Kim, H. D. and Paul, D. R. *Macromolecules* 1992, **25**, 788
- 29 McCall, M. A., Caldwell, J. R., Moore, H. G. and Beard, H. M. *J. Macromol. Sci.-Chem. (A)* 1969, **3**, 911
- 30 de Abajo, J. and de Santos, E. *Angew. Makromol. Chem.* 1983, **111**, 17
- 31 Lee, W. M. *Polym. Eng. Sci.* 1980, **20**, 65
- 32 Bondi, A. J. *Phys. Chem.* 1964, **68**, 441
- 33 van Krevelen, D. W. 'Properties of Polymers: their correlation with chemical structure; their numerical estimation and prediction from additive group contributions', Elsevier, Amsterdam, 1990
- 34 Felder, R. M. and Huvard, G. S. *Meth. Exp. Phys.* 1980, **16c**, 315
- 35 Wonders, A. and Paul, D. J. *Membr. Sci.* 1979, **5**, 63
- 36 Koros, W. J. and Chern, R. T. in 'Membrane Processes - Gas Separations' (Ed. R. W. Rousseau), Wiley, New York, 1987
- 37 Shen, M. C. and Eisenberg, A. *Rubber Chem. Technol.* 1970, **43**, 95
- 38 Lozano, A. E., de Abajo, J., de la Campa, J. G. and Preston, J. *Polymer* 1994, **35**, 872
- 39 Lozano, A. E., de Abajo, J., de la Campa, J. G. and Preston, J. *Polymer* 1994, **35**, 1317
- 40 Jacobson, S. H. *Polym. Prepr.* 1991, **32**(2), 390
- 41 Koros, W. J. *J. Polym. Sci., Polym. Phys. Edn.* 1985, **23**, 1611
- 42 Dine-Hart, R. A. and Wright, W. W. *Makromol. Chem.* 1971, **143**, 189
- 43 Ghosal, K., Chern, R. T., Freeman, B. D. and Savariar, R. *Adv. Filtr. Separ. Technol.* 1993, **7**, 372
- 44 Weinkauff, D. H. and Paul, D. R. *J. Polym. Sci., Polym. Phys. Edn.* 1992, **30**, 837
- 45 Tien, C.-F., Surnamer, A. D. and Patton, S. M., AIChE National Conf. Miami, FL, 1992
- 46 Aitken, C. L., McHattie, J. S. and Paul, D. R. *Macromolecules* 1992, **25**, 2910
- 47 Chung, C. I. and Sauer, J. A. *J. Polym. Sci. (A-2)* 1971, **9**, 1097
- 48 Yee, A. F. and Smith, S. A. *Macromolecules* 1981, **14**, 54
- 49 Lozano, A. E., de la Campa, J. G., de Abajo, J. and Preston, J. *J. Polym. Sci. (A) Polym. Chem.* 1993, **31**, 1383
- 50 Lozano, A. E. Ph.D. Dissertation, Universidad Complutense, Madrid, 1991